

# Evaluation of Spalling in Bridges Using Machine Vision Method

Eslam Mohammed Abdelkader<sup>a,b</sup>, Osama Moselhi<sup>a</sup>, Mohamed Marzouk<sup>b</sup> and Tarek Zayed<sup>c</sup>

<sup>a</sup>Department of Building, Civil, and Environmental Engineering, Concordia University, Canada

<sup>b</sup>Structural Engineering Department, Faculty of Engineering, Cairo University, Egypt

<sup>c</sup>Department of Building and Real Estate, the Hong Kong Polytechnic University, Hong Kong

E-mail: [eslam\\_ahmed1990@hotmail.com](mailto:eslam_ahmed1990@hotmail.com), [moselhi@encs.concordia.ca](mailto:moselhi@encs.concordia.ca), [mm\\_marzouk@yahoo.com](mailto:mm_marzouk@yahoo.com), [tarek.zayed@polyu.edu.hk](mailto:tarek.zayed@polyu.edu.hk)

## Abstract –

The growing number of bridges and their deteriorated conditions on one hand and the budget squeeze for their repair and rehabilitation on the other call for automated detection of defects and smart methods for condition rating of these bridges. This paper presents a newly-developed standalone computer application for automated detection and evaluation of spalling severities in reinforced concrete bridges. The application is coded in C#.net and makes use of an early developed model for detection of surface defects. The method is applied in two tiers, in the first tier, a single-objective particle swarm optimization model is developed for detection of spalling based on Tsallis entropy function. The second tier is devised for evaluation of spalling severities. It generates a comprehensive representation of the bridge deck image using Daubechies discrete wavelet transform feature description algorithm. The second tier also encompasses a hybrid artificial neural network-particle swarm optimization model for accurate prediction of spalling area; circumventing the drawbacks of the gradient descent algorithm. The developed method was tested using 60 images from three bridge decks in Montreal and Laval in Quebec, Canada. Results indicate significant superiority in area prediction accuracies; achieving mean absolute percentage error, mean absolute error and relative absolute error of 6.12%, 56.407 and 0.393, respectively. The developed method is expected to assist transportation agencies in performing more accurate condition assessment of concrete bridge decks and accordingly assist them in developing optimum maintenance plans.

## Keywords –

Image; Reinforced Concrete Bridges; Spalling; Single-objective Optimization; Tsallis entropy; Daubechies discrete wavelet transform; artificial neural network

## 1 Introduction

Bridges are vital elements in infrastructure systems. Meanwhile, they are vulnerable to severe deterioration agents such as freeze-thaw cycles, excessive distress loads due to traffic overload, sulfates, alkali-silica reaction, poor construction practices, etc. It was reported that 26% of the bridges in Canada are experiencing medium to very poor severity levels. They are expected to suffer a further degradation in their condition ratings resulting from the increase of backlog of intervention actions [1-2]. There are two main reasons for the significant deterioration of bridges which are: the decrease in the public investment, and the high age of bridges. The investment in bridges is below the required level to maintain the age of bridges constant, whereas the age of bridges increased by 3.2 years from 21.3 years in 1985 to 24.5 years in 2007. Bridges in Quebec have the highest average age followed by Nova Scotia. Conversely, Prince Edward Island's bridges have the lowest average age. In this context, the average age of bridges on Quebec, Nova Scotia, and Prince Edward Island are 31, 24.5, and 15.6, respectively [3].

In the light of forgoing, it is essential to assess the structural condition ratings of bridges in order to maintain them within acceptable performance levels. The use of machine vision technologies has emerged in the last few years because they enable more efficient and cost effective assessment of structural components than visual inspection. Spalling is an important surface defect that is larger and deeper than scaling. It is created as a result of corrosion of steel reinforcement and it affects the durability and structural integrity of reinforced concrete bridges [4]. In this regard, the present study proposes a novel method for the evaluation spalling in reinforced concrete bridges. It is expected that the developed method will enable decision makers in improving accuracy, reducing cost and minimizing the inherent subjectivity of the visual

inspection process of reinforced concrete bridges.

## 2 Literature Review

Several machine vision-based methods were developed for the purpose of evaluating of surface defects in bridges. Ho et al. [5] developed a method for surface damage detection in cable-stayed bridges. In the developed method, median filter and histogram equalization were applied to improve the quality of captured images. The captured images were then projected onto principal component analysis sub-space. Mahalanobis square distance was then utilized to detect the existence of defects through computing the distance between the projection of input image and all the trained images. Noh et al. [6] proposed a method for the detection of cracks using fuzzy C-means clustering. In it, a set of morphological operations were employed to better reveal the characteristics of cracks and remove noise from the background. This encompassed dilation operation, manually-tuned masks and connected-component labelling. It was highlighted that the developed method could achieve higher recall and precision when compared against other edge detection-based methods.

Mohammed Abdelkader et al. [7] introduced a two-stage multi-objective optimization-based method for the sake of detection of crack images in reinforced concrete bridges. In it, invasive weed optimization algorithm was employed to find the optimum thresholds capitalizing on Kapur entropy function and Renyi entropy function. It was found that the developed method could achieve mean-squared error, peak signal to noise ratio and structural similarity index of 0.0784, 11.4831 and 0.9921, respectively. Talab et al. [8] proposed an approach for the detection of cracks in images based on a combination of edge-detection and histogram-based algorithms. Sobel filter was first applied to detect the edges of crack. Then, Otsu algorithm was utilized to classify the image into cracking pixels and background. It was deduced that the proposed approach could achieve clear and accurate identification of cracks with no noise.

Otero et al. [9] introduced five-stage algorithm for the detection of cracks. Anisotropic diffusion filter was applied to smooth the image while preserving cracking details. Sobel algorithm was utilized to extract cracking edges from the image. The resulted images from Sobel algorithm were processed using active contours technique for the segmentation of cracks. A group of morphological operations were then applied to remove noise blobs. It was highlighted that the developed algorithm could deal with transversal, longitudinal and alligator cracks. Liu et al. [10] presented a method for the detection of cracks in concrete structures

capitalizing on multi-scale enhancement and visual features. Multi-scale enhancement algorithm supervised by gradient information was utilized to filter out noise from the images. A combination of Sobel operator and adaptive threshold segmentation was used to binarize the enhanced images. Closing and small area removal morphological operations were then used to integrate the fragmented cracks and remove the noises. It was found that the developed method could eventually achieve higher true positive rate when compared against Otsu and morphology-based algorithm in addition to percolation model-based algorithm.

Wang et al. [11] introduced an algorithm for crack detection of concrete bridges. In it, adaptive filter of size  $3 \times 3$  was employed multiple times to remove any superimposed noises. Then, contrast enhancement was applied to the processed images to retain detailed information of the target crack as much as possible. An integration of Otsu threshold segmentation and modified Sobel operator were used to detect cracking pixels present in the image. It was inferred that the developed algorithm could achieve absolute error of 0.02 mm in the detection of cracking width. Pavithra et al. [12] developed an image processing-based method for the detection of cracks in concrete structures. Median filter was employed to remove salt and pepper noise that corrupts the images. Threshold segmentation was applied to separate the cracking pixels from the background. Erosion and dilation morphological operations with manually tuned structuring elements were applied to better detection the details of cracks. The outputs from Grey-level co-occurrence matrix alongside statistical features of the images were used as an input to the cascaded random forest classifier for cracking detection. The developed method was able to achieve a detection accuracy of 98%.

Shehata et al. [13] developed two models for the estimation of cracking width using feed and cascade forward back propagation artificial neural network models. Each crack was divided into segments and the maximum width of each segment was computed. It was reported that feed forward back propagation artificial neural network provided higher prediction accuracies achieving mean absolute testing error of 10.3%. Andrushia et al. [14] presented a method for structural concrete crack detection using a combination of image processing algorithms. Anisotropic diffusion filter was first employed to smooth the input images. The filtered images were then fed into the six sigma statistical method to separate the foreground cracking pixels from the background. The developed method outperformed some state of the art methods accomplishing mean squared error, peak signal to noise ratio and mean structural similarity of 62.41, 35.63 and 0.923, respectively. Jain and Sharma [15] proposed an

automatic system for the detection of severity levels of cracks. After applying histogram equalization and contrast enhancement, the processed images were segmented using K-means clustering algorithm. Different settings of K-means clustering were investigated, whereas it was found that random initialization with Euclidean distance provided better results. A fuzzy inference system was then devised for crack risk prediction based on aggregated score.

### 3 Proposed Method

The primary objective of the present study is to develop a computerized platform for the automated detection and severity assessment of spalling in reinforced concrete bridges. This research study extends on a method earlier developed by the authors for the recognition of surface defect type in the image [16]. The flowchart of the proposed method is depicted in Figure 1. In this context, the framework houses five main modules, namely data prep-processing, automated detection, feature extraction, automated evaluation and method validation. It should be mentioned that the spalling detection and assessment of its severities are described and validated separately. In the first module, the input true-color image RGB is transformed to the grayscale image to accelerate the computational process, whereas the intensity values of the gray level image are varying from 0 to 255. The images are resized to 200×200 to better capture the details and characteristics of spalling present in the images.

The performance of machine vision algorithms depends on the quality of the input images which may be corrupted with noise during acquisition and transmission phases. Noise is undesirable random fluctuations in the color and brightness of the image. In this context, the proposed method utilizes Frost filter to remove noises from the input images while retaining the fine details and edges of the object of interest. Frost is an exponentially weighted average filter that employs local statistics to reduce separate and multiplicative noises. It is based on computing an image coefficient of variation which is equal to the ratio of local standard deviation to the local mean of the noisy filter. Frost filter can be mathematically expressed as follows [17-18].

$$R^{\wedge}(\tau) = \sum_{n \times n} K \alpha e^{-\alpha |t|} \quad (1)$$

Such that;

$$\alpha = \frac{4}{n \sigma^{\wedge 2}} \times \frac{\sigma^2}{I^2} \quad (2)$$

$$t = |X - X_o| + |Y - Y_o| \quad (3)$$

Where;

K denotes a normalizing constant.  $\sigma^{\wedge 2}$  stands for the image coefficient of variation.  $\sigma^2$  denotes the local variance. n represents the moving kernel size. I represents the local mean.

Processing of defects images in reinforced concrete bridges is a challenging task because of their complexity, low contrast, color distortion and non-uniform illumination. In this regard, the proposed method utilizes min-max gray level discrimination approach for the sake of improving the contrast of images. This is accomplished through increasing the gray level intensities of the spalling pixels meanwhile decreasing the intensities of the non-spalling pixels [19].

The second module is designated for automated detection of spalling. Image segmentation is one of the basic and critical operations used to analyze the retrieved images in pattern recognition applications. It is the process of dividing the image into non-overlapping multiple segments based on some attributes such as color, intensity and texture. In this regard, optimization-based method proved their efficiency in dealing with complex image segmentation problems in various applications [7]. In the present study, bi-level thresholding is applied to segment the spalling images by designing a single-objective particle swarm optimization model that aims at maximizing Tsallis entropy of the image. The output of this module is a single threshold T that classifies the image pixels into two classes: the spalling (foreground) and surface (background).

The third module is the feature extraction of the captured images. It comprises the use of Daubechies discrete wavelet transform. It decomposes the input original image into four sub-images via high-pass and low-pass filters. The four quadrant sub-bands are called HH<sub>n</sub>, LL<sub>n</sub>, HL<sub>n</sub> and LH<sub>n</sub>. For instance, LL<sub>n</sub> is generated through employing low-pass filter for both rows and columns. LH<sub>n</sub> is generated through employing low-pass filter for rows and high-pass filter for columns [20-21]. The fourth module is the automated assessment of spalling severities. The proposed method (ANN – PSO) utilizes particle swarm optimization algorithm for both parametric and structural training of back propagation artificial neural network. This involves autonomous optimizing the weights of artificial neural network and its best possible architecture. In this context, artificial neural network is trained through formulating a variable-length single-objective optimization problem which encompasses a fitness function of minimization of mean absolute percentage error of spalling area. The optimized artificial neural network is then appended and adopted to simulate the testing dataset for its performance evaluation. Particle swarm optimization algorithm is a widely-recognized meta-heuristic that proved its efficiency in dealing with complex and

diverse optimization problems such as allocation of irrigation water [22], resource-constrained project scheduling [23] and damage detection using vibrational data [24].

The automated detection model is validated through comparison against Otsu algorithm. It is an unsupervised algorithm that is used to segment an image by maximizing the variance between the segmented

classes [25]. The performance of the automated assessment model is evaluated against the back propagation artificial neural network for its validation.



Figure 1. Main modules of the developed spalling detection model

#### 4 Method Development

This section describes the basic computational procedures of Tsallis entropy algorithm and particle swarm optimization algorithm.

##### 4.1 Tsallis Entropy

Assume an image  $I$  that contains  $L$  gray-levels  $\{0, 1, 2, 3, \dots, L - 1\}$ . Tsallis entropy can be defined using Equation (4) [26-27].

$$S_q = \frac{1 - \sum_1^k (P_i)^q}{q - 1} \quad (4)$$

Where;

$k$  represents the total number of possibilities in the system.  $q$  denotes Tsallis entropy or entropic index.

Tsallis entropy of a whole system can be described based on the pseudo additive entropic rule as shown in Equation (5).

$$S_q^{A+B} = S_q^A + S_q^B + (1 - q)S_q^A S_q^B \quad (5)$$

Tsallis entropy of the two classes  $C1$  and  $C2$  can be computed using Equations (6) and (7), respectively. Tsallis entropy is computed based on the calculation of the probabilities of occurrence of the gray levels  $P_i$ , whereas  $\sum_{i=0}^{L-1} P_i = 1$

$$S_q^{C1}(T) = \frac{1 - \sum_{i=0}^{T-1} \left(\frac{P_i}{P^{C1}}\right)^q}{q - 1}, P^{C1} = \sum_{i=0}^{T-1} P_i \quad (6)$$

$$S_q^{C2}(T) = \frac{1 - \sum_{i=T}^{L-1} \left(\frac{P_i}{P^{C2}}\right)^q}{q - 1}, P^{C2} = \sum_{i=T}^{L-1} P_i \quad (7)$$

Where;

$S_q^{C1}(T)$  and  $S_q^{C2}(T)$  represent Tsallis entropy of the two classes  $C1$  and  $C2$ , respectively.

Thus, the objective of the optimization problem is to find the gray threshold  $T$ , which maximizes Tsallis entropy of the segmented classes as per Equation (8).

$$F(T) = \max (S_q^A + S_q^B + (1 - q)S_q^A S_q^B) \quad (8)$$

##### 4.2 Particle Swarm Optimization

Particle swarm optimization is a population-based meta-heuristic that was first introduced by Eberhart and Kennedy. The basic computational stages of particle swarm optimization algorithm are depicted in Figure 2 [28-29]. It is inspired by the social behaviour of migrating flock of birds. Each candidate solution is called “particle” and a population of randomly positioned particles in the search space is called “swarm”. Each particle in the multi-dimensional solution space is characterized by its position and velocity. During each iteration in the evolution process, each particle monitors its current position, the best position it achieved and its own flying velocity. The position and velocity of each particle is updated according to its own best flying experience and the best position achieved by the entire swarm. In this regard, the position of the best particle in the swarm is obtained based on the pre-defined fitness function(s). The computational procedures of particle swarm optimization algorithm combines local and global search which helps in providing a proper balance between exploration and exploitation. The positions and velocities of the swarm of particles in the trajectory are updated as follows.

$$v_i(t + 1) = w \times v_i(t) + c_1 \times r_1 \times (pbest_i(t) - x_i(t)) + c_2 \times r_2 \times (gbest(t) - x_i(t)) \quad (9)$$

$$x_i(t + 1) = x_i(t) + v_i(t + 1) \quad (10)$$

Where;

$x_i(t)$  and  $x_i(t + 1)$  denote the position of the  $i$ -th particle in iteration  $t$  and  $t + 1$ , respectively.  $v_i(t)$  and  $v_i(t + 1)$  represent the velocity of the  $i$ -th particle in iteration  $t$  and  $t + 1$ , respectively.  $pbest_i$  is the individual local best position that particle  $i$  achieved so far.  $gbest$  stands for the global best position achieved by the entire swarm.  $c_1$  and  $c_2$  are two acceleration coefficients that denote cognitive learning, and social parameters, respectively. They enable controlling the global and local guides.  $r_1$  and  $r_2$  represent two uniformly distributed random numbers searching for better solutions along the direction towards the personal best and global best.  $w$  refers to the inertia weight. It is advised to start with a large inertia factor and then it decreases within the evolution process to enable both global and local explorations.

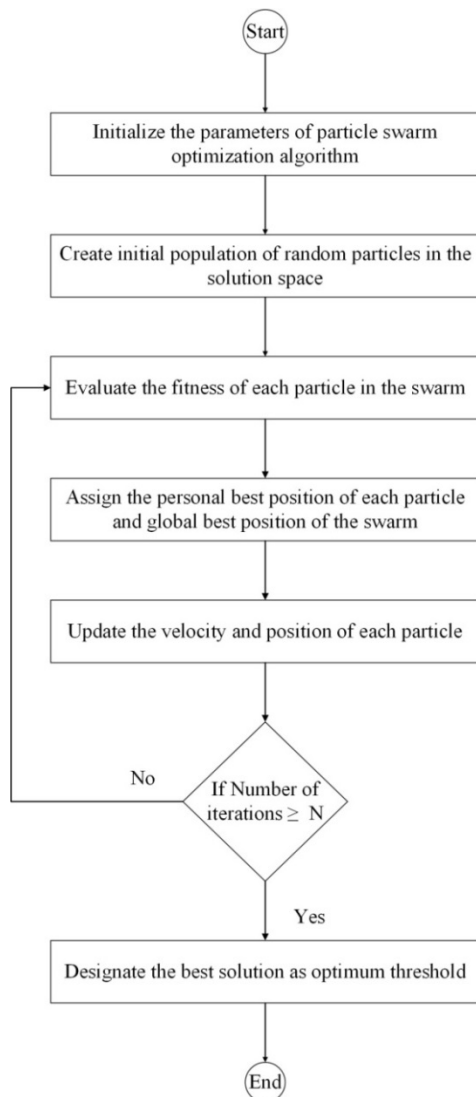
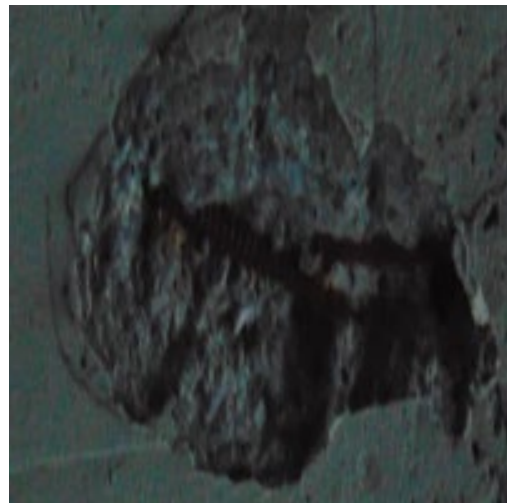


Figure 2. Flowchart of particle swarm optimization algorithm

## 5 Method Implementation

A dataset comprising of 60 real-world images are used as an input to experiment the proposed method such that 50 images are used for training while the remaining 10 images are used for testing. These images are captured from bridge decks in Montreal and Laval, Canada using Sony DSC-H300 digital camera of 20.1 megapixel resolution. All the calculations and optimization algorithms took place on a laptop with an Intel Core i7 CPU, 2.2 GHz and 16 GB of memory. Sample of the spalling images used is presented in Figure 3.



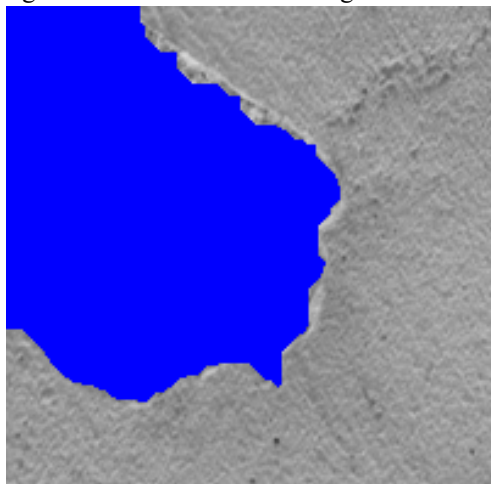
(a) Image "A"



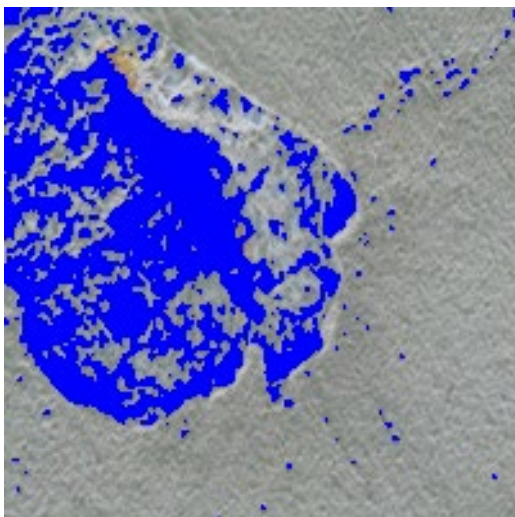
(b) Image "B"

Figure 3. Sample of the spalling images

In the automated spalling detection model, Tsallis entropy index is assumed 0.5. With respect to the particle swarm algorithm in this model, the number of iterations and the initial population size are assumed 30 and 10, respectively. The cognitive learning and social parameters are assumed 2 while the inertia factor is assumed 0.5. Figure 4 demonstrates the segmented image of spalling after the application of the single objective particle swarm optimization-based segmentation method alongside the segmented image after the implementation of Otsu algorithm. As can be seen, the developed detection model successfully recognized the spalling. However, Otsu algorithm failed to discriminate the spalling pixels from the background causing a lot of distortion in the image.



(a) Segmented image using the developed detection model



(b) Segmented image using Otsu algorithm

Figure 4. Visual representation of spalling detection models

At the level of spalling evaluation, the ANN – PSO model is composed of one output neuron for the prediction of spalling area. The optimization parameters of the developed ANN – PSO model are recorded in Table 1. It is found that the optimum numbers of hidden layers and hidden neurons are one and two, respectively. Tangent sigmoid is the optimum transfer function. A comparative analysis between the ANN – PSO model and the back propagation artificial neural network is presented in Table 2. The comparison is carried out using mean absolute percentage error (MAPE), mean absolute error (MAE) and relative absolute error (RAE). It can be inferred that the developed assessment model substantially outperformed the conventional artificial neural network through reducing MAPE, MAE and RAE by 76.65%, 71.47% and 71.43%, respectively.

Table 1. Optimization parameters of the developed

ANN – PSO model	
Parameter	Corresponding value
Minimum number of hidden layers	1
Minimum number of hidden neurons	1
Maximum number of hidden layers	10
Maximum number of hidden neurons	10
Initial population size	200
Number of iterations	400
Cognitive learning	2
Social parameter	2
Inertia weight	0.5

Table 2. Performance comparison between the spalling evaluation models

Model	MAPE	MAE	RAE
ANN – PSO	6.12%	56.407	0.393
Artificial neural network	26.21%	197.756	1.376

## 6 Conclusion

Routine visual inspections are mandatory to build condition assessment models. Nevertheless, they are prone to subjective judgments. This can lead to inaccurate deterioration models and intervention actions. In this context the present study introduces a novel two-tier method for the automated detection and evaluation of spalling in reinforced concrete bridges.

Results obtained from the visual comparison demonstrated superiority of the spalling segmentation model of the developed method. It was able to establish

well-separated thresholds as well as more compact and homogenous clusters. On the other hand, Otsu algorithm failed to detection spalling pixels in the image. With regard to the spalling evaluation, it was concluded that the developed spalling evaluation model managed to reduce of the prediction error by values ranging from 71.43% to 76.65% with reference to the artificial neural network. Accordingly, the developed method can be deployed as an efficient tool to provide safer, productive and more reliable inspection of reinforced concrete bridges.

## References

- [1] Felio, G. Canadian Infrastructure Report Card. Canadian Construction Association, Canadian Public Works Association, Canadian Society for Civil Engineering, and Federation of Canadian Municipalities, Canada. <[www.canadainfrastructure.ca/downloads/Canada\\_n\\_Infrastructure\\_Report\\_2016.pdf](http://www.canadainfrastructure.ca/downloads/Canada_n_Infrastructure_Report_2016.pdf)> (06.05.2016), 2016.
- [2] Mohammed Abdelkader, E., Moselhi, O., Marzouk, M. and Zayed, T. Condition Prediction of Concrete Bridge Decks Using Markov Chain Monte Carlo-Based Method, *7th CSCE International Construction Specialty Conference Jointly with Constrction Research Congress*, Canada, 1-10, 2019.
- [3] Viami International Inc. and the Technology Strategies Group. *Market Study for Aluminium Use in Roadway Bridges*, 1-29, Montreal, Canada, 2013.
- [4] Mazzotta, F., Lantieri, C., Vignali, V., Simone, A., Dondi, G. and Sangiorgi, C. Performance evaluation of recycled rubber waterproofing bituminous membranes for concrete bridge decks and other surfaces. *Construction and Building Materials*, 136:524–532, 2017.
- [5] Ho, H., Kim, K., Park, Y. and Lee, J. An efficient image-based damage detection for cable surface in cable-stayed bridges. *NDT & E International*, 58:18–23, 2013.
- [6] Noh, Y., Koo, D., Kang, Y. M., Park, D. G. and Lee, D. H. Automatic crack detection on concrete images using segmentation via fuzzy C-means clustering. *Proceedings of the 2017 IEEE International Conference on Applied System Innovation: Applied System Innovation for Modern Technology*, Japan, 877-880, 2017.
- [7] Mohammed Abdelkader, E., Moselhi, O., Marzouk, M. and Zayed, T. A Multi-objective Invasive Weed Optimization Method for Segmentation of Distress Images *Intelligent automation and soft computing*, 1-20, 2019.
- [8] Talab, A. M. A., Huang, Z., Xi, F. and Haiming, L. Detection crack in image using Otsu method and multiple filtering in image processing techniques. *Optik*, 123:1030–1033, 2016.
- [9] Otero, L. D., Moyou, M., Peter, A. and Otero, C. E. Towards a Remote Sensing System for Railroad Bridge Inspections: A Concrete Crack Detection Component. *Proceedings of IEEE SOUTHEASTCON*, United States of America, 1-4, 2018.
- [10] Liu, X., Ai, Y. and Scherer, S. Robust Image-based Crack Detection in Concrete Structure Using Multi-scale Enhancement and Visual Features. *2017 IEEE International Conference on Image Processing*, China, 2304-2308, 2017.
- [11] Wang, Y., Zhang, J. Y., Liu, J. X., Zhang, Y., Chen, Z. P., Li, C. G., He, K. and Yan, R. Research on Crack Detection Algorithm of the Concrete Bridge Based on Image Processing. *Procedia Computer Science*, 154:610–616, 2018.
- [12] Pavithra, D., Saranya, T., Prakash, K. and Soundarya, G. Electronic Crack Detection On Concrete. *International Journal of Advanced Science and Engineering Research*, 3:515–521, 2018.
- [13] Shehata, H. M., Mohamed, Y. S., Abdellatif, M. and Awad, T. H. Crack width estimation using feed and cascade forward back propagation artificial neural networks. *Key Engineering Materials*, 786:293–301, 2018.
- [14] Andrushia, D., Anand, N. and Arulraj, P. Anisotropic diffusion based denoising on concrete images and surface crack segmentation. *International Journal of Structural Integrity*, 11:395–409, 2019.
- [15] Jain, R. and Sharma, R. S. Predicting Severity of Cracks in Concrete using Fuzzy Logic. *International Conference on Recent Innovations in Electrical, Electronics and Communication Engineering*, India, 2976–2982, 2018.
- [16] Mohammed Abdelkader, E., Moselhi, O., Marzouk, M. and Zayed, T. (2020). “Hybrid Elman Neural Network and Invasive Weed Optimization Method for Bridge Defects Recognition, *Submitted to: Journal of the Transportation Research Board*.
- [17] Kulkarni, S., Kedar, M. and Rege, P. P. Comparison of Different Speckle Noise Reduction Filters for RISAT-1 SAR Imagery. *International Conference on Communication and Signal Processing*, India, 537-541, 2018.
- [18] Dhanushree, M., Priyadharsini, P., Sharmila, T. S. Acoustic image denoising using various spatial filtering techniques. *International Journal of Information Technology*, 11:659-665, 2019.

- [19]Hoang, N. Detection of Surface Crack in Building Structures Using Image Processing Technique with an Improved Otsu Method for Image Thresholding, *Advances in Civil Engineering*, Article ID 3924120, 10 pages, 2018.
- [20]Waqas, U. A., Khan, M. and Batool, S. I. A new watermarking scheme based on Daubechies wavelet and chaotic map for quick response code images. *Multimedia Tools and Applications*, 79:6891–6914, 2020.
- [21]Devi, T. K. and Sakthivel, P. Pipelined Direct Mapping Method based Low Power VLSI Architecture for the 4-Tap Wavelet Filter. *Asian Journal of Applied Science and Technology*, 1:76–79, 2017.
- [22]Noory, H., Liaghat, A. M., Parsinejad, M. and Haddad, O. B. Optimizing Irrigation Water Allocation and Multicrop Planning Using Discrete PSO Algorithm. *Journal of Irrigation and Drainage Engineering*, 138:437–444, 2012.
- [23]Koulinas, G., Kotsikas, L. and Anagnostopoulos, K. A particle swarm optimization based hyper-heuristic algorithm for the classic resource constrained project scheduling problem. *Information Sciences*, 277:680–693, 2014.
- [24]Kang, F., Li, J. J. and Xu, Q. Damage detection based on improved particle swarm optimization using vibration data. *Applied Soft Computing Journal*, 12:2329–2335, 2012.
- [25]Khairuzzaman, A. K., and Chaudhury, S. Multilevel Thresholding using Grey Wolf Optimizer for Image Segmentation. *Expert Systems With Applications*, 86:64–76, 2017.
- [26]Mishra, S., and Panda, M. Bat Algorithm for Multilevel Colour Image Segmentation Using Entropy-Based Thresholding. *Arabian Journal for Science and Engineering*, 43(12):7285-7314, 2018.
- [27]Bhandari, A. K., Kumar, A., and Singh, G. K. Tsallis Entropy Based Multilevel Thresholding for Colored Satellite Image Segmentation using Evolutionary Algorithms. *Expert Systems With Application*, 42(22):8707-8730, 2015.
- [28]Kennedy, J. and Eberhart, R. Particle swarm optimization. *Proceedings of the IEEE International Conference on Neural Networks*, Australia, 1942–1948, 1995.
- [29]Li, F., Gong, Y., Cai, L., Sun, C., Chen, Y., Liu, Y. and Jiang, P. Sustainable land-use allocation: A multiobjective particle swarm optimization model and application in Changzhou, China. *Journal of Urban Planning and Development*, 144:1-11, 2018.